

# INTERPRETATION OF THE CORONAL EUV SIGNATURE OF THE CME EVENT ON JUNE 27 1999

N.-E. Raouafi<sup>1,\*</sup>, S. Mancuso<sup>2</sup>, S. K. Solanki<sup>1</sup>, B. Inhester<sup>1</sup>, C. Benna<sup>2</sup>, J. P. Delaboudinière<sup>3</sup>, G. Stenborg<sup>4</sup>, and M. Mierla<sup>1</sup>

<sup>1</sup>Max-Planck-Institut für Aeronomie, 37191 Katlenburg-Lindau, Germany

<sup>2</sup>INAF, Osservatorio Astronomico di Torino, I-10025 Pino Torinese, Italy

<sup>3</sup>Institut d'Astrophysique Spatiale, F-91405 Orsay, France

<sup>4</sup>The Catholic University of America, Washington DC, USA

## ABSTRACT

We report the observation of a Coronal Mass Ejection (CME) detected on June 27 1999 by the UltraViolet Coronagraph Spectrometer (UVCS) telescope operating on board the SOHO spacecraft. The CME, whose leading edge was expanding at a projected speed of about  $1200 \text{ km s}^{-1}$ , was observed in white light by the Large Angle Spectroscopic Coronagraph (LASCO). The UVCS spectra reveal excess broadening of the O VI doublet lines and enhancement in the intensity of the Si XII lines due to the motion of expanding hot material. The evolution of the UVCS structure is highly correlated to the evolution of the CME observed by LASCO in white light, so that the hot gas emission could be attributable to the passage of a shock wave propagating just in front of the fast CME.

Key words: Plasmas – Coronal Mass Ejections (CMEs) – Flares – Corona – UV radiation – Shock waves.

## 1. INTRODUCTION

Coronal Mass Ejections are usually related to flares and prominence eruptions but some CMEs appear to be unconnected to these solar events (Klassen et al 1999). Priest (1984) points out that the eruption of huge quiet-sun prominences could generate shock waves propagating ahead of the ejected material and violent solar flares could produce shock waves which are revealed by radio emission of accelerated particles of Type II bursts. Fast coronal mass ejections (CMEs), with speeds greater than the Alfvén speed of the local plasma, generate waves, which propagate in front of the cooler CME material. Shock waves can accelerate light (electrons) as well as heavy (ions) coronal particles. Sheeley (2000) found that fast Type II radio bursts, which are considered to be a signature of coronal shock waves, are often associated with large-scale coronal mass ejections (see also Gold

1955). However, the source(s) of coronal shock waves is (are) not yet completely clear. This is because the relation between flares, CMEs and coronal Type II radio bursts is still not understood very well. One reason is that they (shock waves) are difficult to detect except by radio bursts. The source region of these bursts is, however, often difficult to localize.

Extreme ultraviolet spectral observations can provide new and unique insights into the physics of CMEs observed by LASCO and EIT aboard SOHO. These two instruments image the evolution and morphology of CMEs in two dimensions. Ultraviolet spectral analysis with sufficiently high spectral resolution can extend the study of CME evolution into the third dimension through Doppler shift analysis. The Doppler shifts are particularly important for investigating the helical motions expected from some flux rope models of CMEs (e.g. Krall et al. 2001) and can provide useful dynamical constraints on other CME models (Antiochos et al. 1999). Moreover, UV diagnostics allow for density and temperature diagnostics, yielding a means for distinguishing between hot and cold material through the analysis of the intensity of different emission lines.

UVCS observations of CMEs usually show emission in low to moderate ionization stages, while the emission of higher charged ions becomes fainter or remains unchanged (Raymond 2002). In some cases, UV spectra show emission from higher ionization states that can be interpreted as emission from collisionless shock waves detected in connection with the CME eruption (Raymond et al. 2000; Mancuso et al. 2002) or related to reconnection current sheets (Ciaravella et al. 2002). This paper is devoted to the analysis of a CME observed by UVCS on June 27 1999. The peculiarity of this event is related to the propagation of a hot structure detected in the Si XII emission line along the slit positioned at  $2.55 R_{\odot}$ . The Si XII emission is apparently related to an opening loop connected to a simultaneous CME eruption observed by both EIT on the disk and LASCO off the limb. The event was also accompanied by a shock wave, that was detected as a type II radio burst by radio spectrographs.

\* Associated researcher to the LERMA Department at the Observatoire de Paris-Meudon, France

## 2. OBSERVATIONS AND DATA ANALYSIS

The results discussed in the present paper have been obtained from observations made on 1999 June 27 by different instruments aboard the SOHO spacecraft (Solar and Heliospheric Observatory: Domingo et al. 1995). The analysis of this event also relies on radio spectra recorded by the decametric array of Nancay (France) and the Izmiran radio spectrograph (Russia) in addition to information obtained by the Soft X-Ray Telescope on board Yohkoh (Yohkoh/SXT).

### 2.1. UVCS observations

The Ultraviolet Coronagraph Spectrometer (UVCS) measures the intensities and profiles of ultraviolet emission lines in the corona along a slit, which is placed between 1.5 and 10  $R_{\odot}$  from Sun center (Kohl et al. 1995 & 1997). Coronal spectra are acquired in two spectrometer channels: the Ly $\alpha$  channel, which covers the range of 1160 to 1350 Å and the O VI channel, covering the range of 940 – 1123 Å. Our observations utilized the O VI channel that is optimized for the study of the O VI doublet  $\lambda 1031.92$  and  $\lambda 1037.61$ .

The UVCS observation sequence discussed here began on June 26 1999 at 22:26 UT and finished on June 27 at 15:01 UT. The slit was located in the north-western part of the solar corona at 330 degrees counterclockwise from the north pole. Spectra were obtained for different heliocentric distances between 2.0 and 3.09  $R_{\odot}$ . In order to obtain good statistics, different exposure times and slits with different widths were used at different altitudes. For the O VI channel, in order to reduce the noise the obtained spectra were binned by two pixels per bin in the spectral direction and by 6 pixels per bin in the spatial direction. Four wavelength domains were recorded at each exposure: the first wavelength range contains H I Ly $\beta$   $\lambda 1025$ , the O VI doublet  $\lambda 1031.92$  and  $\lambda 1037.61$  and Si XII  $\lambda 520.66$ ; the second one contains the Si XII  $\lambda 499.37$  line (the Si XII lines are observed in second order in the O VI channel); the third range contains H I Ly $\alpha$   $\lambda 1215.67$  and the fourth range contains Mg  $\lambda 609.76$ .

In the data reduction we followed the standard techniques described by Kohl et al. (1997 & 1999). We used the new version DAS33 of the UVCS Data Analysis Software for wavelength and intensity calibration, and removal of image distortion. The uncertainties in the O VI line intensities are due to photon counting statistics, background subtraction, and radiometric calibration.

Of particular interest are three exposures made at 2.55  $R_{\odot}$  from Sun centre shown in Figure 1. These exposures are remarkable because they reveal emission in Si XII (Si XII doublet lines  $\lambda 520.66$  and  $\lambda 499.37$ ), which is rare in CMEs. These lines are present significantly above the noise only along a small part of the slit (lying between the horizontal white bars in Figure 1 for  $\lambda 520.66$ ). The spatial locations of the emission of Si XII  $\lambda 499.37$  on the slit coincide with that of Si XII  $\lambda 520.66$ . By following the location of Si XII emission it is possible to

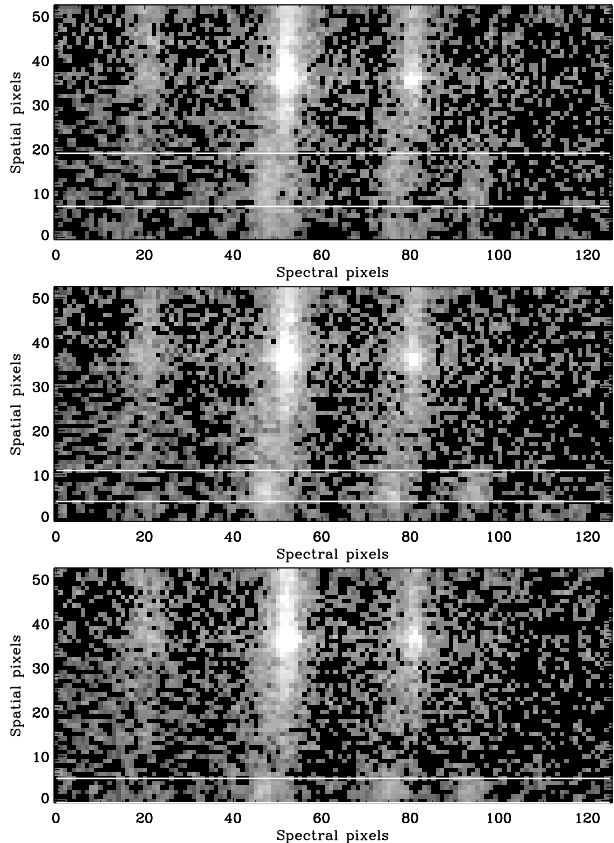


Figure 1. The three UVCS exposures on which the hot gas emission is seen. The spectral lines shown are H I Ly- $\beta$   $\lambda 1025$  (around pixel 20), the O VI doublet  $\lambda 1032$  and  $\lambda 1037$  (around pixels 50 and 75, respectively) and the Si XII  $\lambda 520.66$  line (around pixel 95). The location of the hot gas emission is indicated by two horizontal lines on each panel. The observed structure is responsible for a local intensity enhancement of the O VI doublet lines and also of the emission of the Si XII  $\lambda 520.66$  line. This structure is propagating toward the lower part of the slit (propagation towards the north pole in the corona).

observe the propagation of hot gas along the UVCS slit toward its lower end (corresponding to the north direction in the corona). These exposures were obtained respectively from 09:05 to 09:15 UT, 09:15 to 09:25 UT, and 09:25 to 09:35 UT with an exposure time of 600 seconds each. This moving hot gas is accompanied by a co-spatial intensity enhancement and broadening of the O VI doublet lines ( $\lambda 1031.92$  and  $\lambda 1037.61$ ).

In Figure 2 we plot the average of the three UVCS spectra integrated over the spatial pixels exhibiting enhanced Si XII emission. The two O VI lines are distinctly asymmetric, exhibiting extended wings towards longer wavelengths. They have therefore been fitted by two Gaussians plus background each, while we used a single Gaussian plus background for each of the Si XII lines. The full fit (solid lines) as well as the individual Gaussians are plotted in Figure 2.

The total intensity ratio of the O VI doublet lines, i.e. the ratio of the area under each spectral line, obtained after subtracting the continuum, is equal to 1.86. Inten-

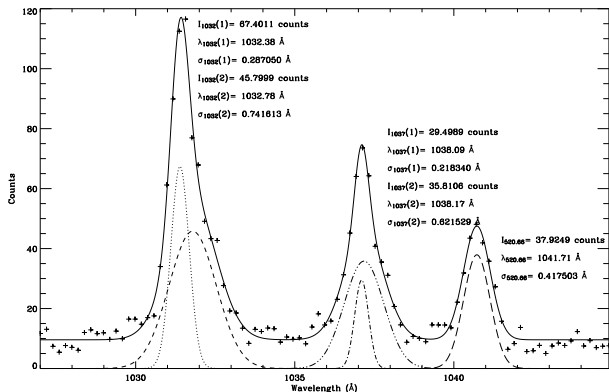


Figure 2. Spectra integrated over the spatial pixels where the intensity enhancement was detected in the UVCS observations for the three exposures shown in Figure 1 (signs +). The solid curve is a fit of the observed-averaged spectrum by Gaussian functions. The O VI lines are fitted by two Gaussians each and the Si XII line by one Gaussian. The Doppler shifts of the different components (narrow and broad components) of the O VI doublet are not equal to the atomic separation of the two lines. This is due to the quality of the signal and to the fit.

sity ratios lower than 2 are only obtained when the O VI  $\lambda 1037.61$  line is subject to the optical pumping due to the C II lines at  $\lambda 1036$ . This occurs for high Doppler shifts. However, the intensity ratio of the two narrow components (dotted profiles in Figure 2) is equal to 2.99, while that of the wide components (dot-dashed profiles) is equal to 1.53. This last value corresponds to speeds of about  $300\text{--}400\text{ km s}^{-1}$  for the O VI ions (see Patsourakos & Vial 2000 and Li et al. 1998), suggesting that the broad component is associated with moving gas, i.e. with the CME. The visible Doppler shift between the broad and narrow components is about  $\sim 50\text{--}100\text{ km s}^{-1}$  which corresponds to the net line-of-sight component of this motion. The quality of the fit affects these values that can be higher. The narrow components of the O VI lines are due to the background-foreground corona contribution along the line of sight. They have line widths and intensity ratios comparable with those at the same positions along the slit before the CME. Note that the last frame recorded prior to the first appearance of the Si XII emission (08:50–09:05 UT) shows a small sign of a broad component in the O VI lines but it is far less conspicuous as in the three following exposures (Figure 1).

In order to obtain a better picture of the whole event we next consider series of EIT/SoHO and LASCO/SoHO images.

## 2.2. EIT and LASCO observations

A soft X-ray flare (M10) was observed by GOES to start at 8:34 UT (with maximum intensity at 8:44 UT) in the active region AR 8592, located at N23 W25. EIT images obtained on June 27 1999 from 6:00 UT to 12:00 UT have been examined to check if this event is related to the ejection of the CME deduced from UVCS observations and

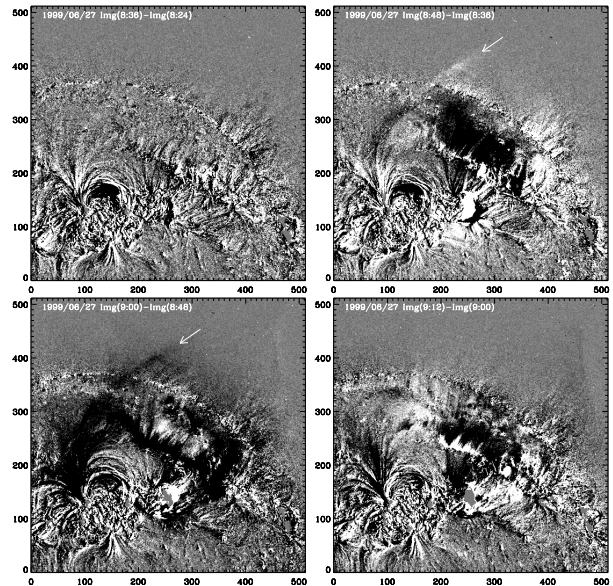


Figure 3. Difference between consecutive EIT  $\lambda 195$  images showing the onset of the CME as well as the eruption of a system of loops to which the structure observed by UVCS seems to be related. The erupting loop system is indicated by arrows on the second and the third panels.

if there were other events in the same region. To better reveal variable and dynamic events we form differences between consecutive EIT  $\lambda 195$  images, plotted in Figure 3. The image difference shows that there are two independent dynamic features. Firstly, the CME observed at solar coordinates  $(338^\circ, 86^\circ)$  roughly corresponding to pixel coordinates  $(240, 140)$  in Figure 3. Secondly, the eruption of a system of loops. On the second panel of Figure 3, this feature is visible as a bright structure, while in the third panel of the same figure it is visible as a dark structure (shown by white arrows). This combination suggests that the off-limb part of the opening loop was only visible on one EIT image, namely the one made at 8:48 UT. This implies that this loop either whipped past or faded very rapidly. Assuming that it had left the field of view within the time between 2 images (12 minutes) we obtain a lower limit for its speed of more than  $700\text{ km s}^{-1}$  (assuming it to be traveling radially outwards from the Sun). This value is consistent with the speed deduced from the UVCS data (broad component of the O VI lines). Actually, taking the location and time of the disturbance on the EIT image and assuming it to travel radially outwards, it would cross the UVCS slit at the time of the first exposure showing enhanced Si XII emission, if it were traveling radially at more than  $1000\text{ km s}^{-1}$ . The observed motion of the opening loop system and of the CME material is affected by projection effects due to the motion out of the plane of the sky. Thus, a  $15^\circ$  error in the direction of the propagation leads to a  $\sim 50\text{ km s}^{-1}$  error in the propagation speed.

According to the CME catalogue, the coronagraph C2 of LASCO detected the CME material of the erupting filament at about 9:06 UT over the north pole. The central position angle of the eruption was around 349 degrees counterclockwise with respect to the north, with a

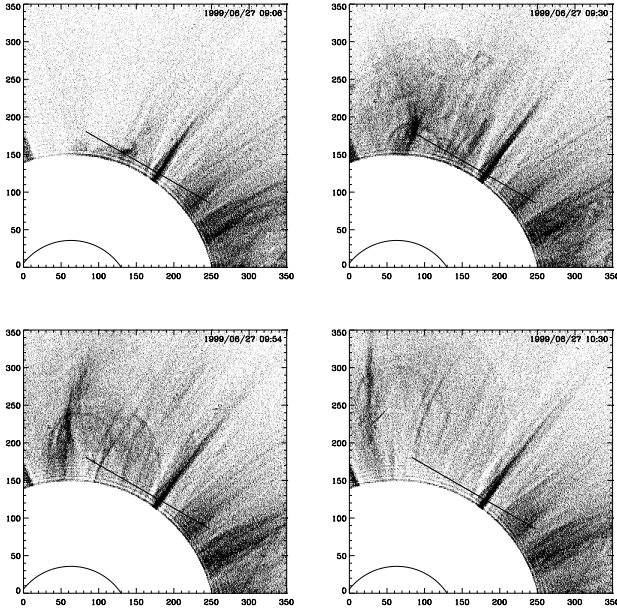


Figure 4. LASCO C2 coronagraph images giving the spatial evolution of the erupted system of loops as well as the CME material observed in white light. The images have been sharpened using wavelet packets (Stenborg and Cobelli, 2003).

full angular width of  $86^\circ$ . Figure 4 shows the evolution of the ejected material as observed by LASCO. In white light, we can observe a structure propagating toward the north pole. In addition, there are also signs of an expanding halo, with a seemingly radial propagation direction. LASCO difference images show an enhancement of the brightness of the streamer belt at the same moment, but no deflection. This structure observed in white light propagating toward the north pole has the same general characteristics of propagation as the Si XII emission along the UVCS slit. At the same time, the curved shape of the white light brightening (see last frame of Figure 4) is similar to that of the opening loop detected earlier by EIT (but with a different inclination with respect to the polar axis). Also, its direction of motion corresponds to the one expected for an opening system of loops. Thus, the hot UVCS structure may be related to the eruption of the system of hot loops.

The speed of the CME was obtained from the online SoHO/LASCO CME catalogue (Yashiro et al. 2002), in which CME kinematics are estimated and compiled from LASCO C2 and C3 images. The CME speed projected on the plane of the sky, estimated from a linear fit to the height-time measurements, is found to be about  $900 \text{ km s}^{-1}$ . However, according to the data base a quadratic fit produces a much better fit to the LASCO sequence and extrapolation to 2.55 solar radii yields a speed of about  $1180 \text{ km s}^{-1}$ . Here we need to pay attention to the projection effect because the speeds listed in the catalogue are derived from the images projected on the sky plane. Consequently, we can assume that the CME speed must have been somewhat higher than about  $1200 \text{ km s}^{-1}$ , making it a fast CME. The estimated speed is at odds with the speed of the hot feature observed by UVCS, even taking

into account possible projection effects.

### 2.3. Radio observations

On 1999 June 27, the Nancy Decameter Array (France) detected a type II radio burst between 08:42 and 08:51 UT in the frequency range of 20-70 MHz. Type II radio bursts appear as bands of enhanced radio emission slowly drifting from high to low frequencies in dynamic radio spectra. These bands are considered to be the signature of the associated shock wave traveling outwards in the corona. The same event was also observed by the Izmiran radio spectrograph (Russia) at about the same time between 08:41 and 08:51 UT in the frequency range between 45 and 130 MHz. Although the fundamental and harmonic lane were not clearly discernable due to the concomitant presence of a type IV radio burst and a noise storm, it was possible to obtain a rough estimate of the shock speed of about  $1000 \text{ km s}^{-1}$  (R. Gorgutsa, private communication). This speed is consistent with the observed speed of the leading edge of the CME mentioned above, implying that the shock could be piston-driven. A fast MHD mode shock may also explain the observations. However, an exact estimate of the shock speed and its relation with the CME is beyond the scope of the present study.

## 3. DISCUSSION

The feature observed propagating along the UVCS slit in EUV (Extreme Ultraviolet) lines (O VI doublet and Si XII) is characterized by line broadening and excess emission of lines with high formation temperature. This is in addition to Doppler shifts of these lines with respect to the foreground-background coronal emission. The emission of the Si XII line indicates the presence of hot material or that a heating mechanism is acting on the plasma in the observed region. This latter could be also the source of the line broadening observed for the O VI lines.

According to the evolution of the inclination angle of the opened loop and the radial distance of the bright bubble upper extremity, it seems that EIT and LASCO were observing the same structure at different altitudes and different times. Note that, assuming a radial motion on the plane of the sky, the speed of the bright structure initially exceeds  $1000 \text{ km s}^{-1}$ . One expects the creation of a shock wave in front of this very fast material traveling along the flux rope. Note also the existence of fast acceleration of the opened loop at the beginning of the event, followed by a deceleration, as deduced from the evolution of radial distance of the bright bubble.

The EUV structure is correlated spatially and temporally to visible observations done by LASCO. Figure 5 shows the temporal and spatial evolution of the Si XII feature observed by UVCS (solid curves) and that of the CME material observed by the coronagraph C2 of LASCO (dashed curves). These curves give the brightness along the UVCS slit (see Figure 5) of the Si XII  $\lambda 520.66$  line (for UVCS observations) and the white light brightness

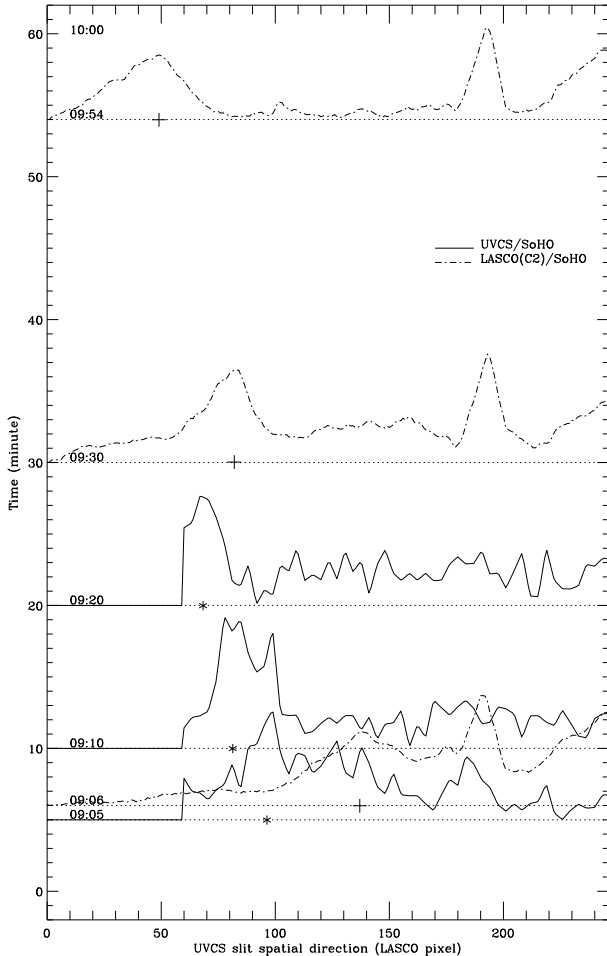


Figure 5. Evolution of the spatial distribution of brightness. The solid curves represent Si XII intensity along the slit in the three UVCS exposures (see Figure 1). Vertical location of each curve corresponds to the time at which the data were recorded. The visible-light brightness recorded by LASCO C2 at three different times along the UVCS slit (see Figure 1) is represented by the dot-dashed curves. The left of the Figure extends beyond the UVCS slit in order to allow the brightness peak in the LASCO image taken at 9:54 to be plotted. Symbols (\*) and (+) display the maxima of the time-dependent emission of the Si XII  $\lambda 520.66$  and of white light, respectively. Clearly, the hot gas (UVCS) is propagating just in front of the colder material (LASCO).

(LASCO observations). The fixed feature in the right parts of the dashed (i.e. LASCO) curves correspond to the narrow streamer crossing the right half of the UVCS slit. The feature observed in the EUV line and that observed in white light are both propagating in the same direction (toward the left part of the panel, which corresponds to the north pole direction). This evolution shows that the EUV feature is propagating just in front of the opening loop.

#### 4. CONCLUSIONS

We report on a CME observed on June 27 1999 by the UVCS telescope. Emission of hot material has been ob-

served by UVCS propagating in front of an opening system of loops simultaneously with a CME. The evolution of the UVCS structure was found to be highly correlated to the evolution of the opened loop observed by LASCO. The peculiarity of this event is related to the propagation of a hot structure detected along the slit positioned at 2.55 solar radii in the Si XII emission line that seems to be related to an opening loop observed in connection to a simultaneous CME eruption by both EIT and LASCO on the disk. The broadening of the O VI doublet lines and the enhancement of the Si XII  $\lambda\lambda 520.66$  and  $499.37$  lines was due to the expanding hot gas. The event was also related to a shock wave, detected as a type II radio burst by radio spectrographs.

#### ACKNOWLEDGMENTS

We thank Roman Gorgutsa of the Izmiran radio spectrograph (Russia) for providing us a figure of the dynamic spectra of the type II radio burst and for his useful comments. The CME catalog is generated and maintained by the Center for Solar Physics and Space Weather, The Catholic University of America in cooperation with the Naval Research Laboratory and NASA. SOHO is a project of international cooperation between ESA and NASA.

#### REFERENCES

- Antiochos, S. K., MacNeice, P. J., Spicer, D. S., & Klimchuk, J. A. 1999, *ApJ*, 512, 985
- Ciaravella, A., Raymond, J. C., Li, J., Reiser, P., Gardner, L. D., Ko, Y.-K., & Fineschi, S. 2002, *ApJ*, 575, 1116
- Domingo, V., Fleck, B., & Poland, A. I. 1995, *Solar Phys.*, 162, 1
- Gold, T. 1955, Discussion of shock waves and rarefied gases, in *Gas Dynamics of Cosmic Clouds*, edited by J. C. van de Hulst and J. M. Burgers, North-Holland Publishing Co., Amsterdam, p.103
- Klassen, A., Karlický, M., Aurass, H., Jiricka, K. 1999, *Solar Phys.*, 188, 141-154
- Kohl, J. L., Esser, R., Gardner, L. D., et al. 1995, *Solar Phys.*, 162, 313
- Kohl, J. L., Noci, G., Antonucci, E., et al. 1997, *Solar Phys.*, 175, 613
- Kohl, J. L., Esser, R., Cranmer, S. R., et al. 1999, *ApJ*, 510, L59
- Krall, J., Chen, J., Duffin, R. T., Howard, R. A., & Thompson, B. J. 2001, *ApJ*, 562, 1045
- Li, X., Habbal, S. R., Kohl, J., & Noci, G. 1998, *ApJL*, 501, L133
- Mancuso, S., Raymond, J. C., Kohl, J., Ko, Y.-K., Uzzo, M., & Wu, R. 2002, *A&A*, 383, 267
- Priest, E. R. 1984, *Solar Magnetohydrodynamics*, Geophysics and Astrophysics Monographs, D. Reidel Publishing Company

Raymond, J. C., Thompson, B. J., St. Cyr, O. C., Gopalswamy, N., Kahler, S., Kaiser, M., Lara, A., Ciaravella, A., Romoli, M., & O'Neal, R. 2000, *Geophys. Res. Lett.*, 27, 1439

Raymond, J. C., 2002, *Proceedings SOHO 11 Symposium*, ESA SP-508, 421

Sheeley, N. R., Jr., Hakala, W. N., Wang, Y.-M. 2000, *J. Geo. Res.*, 105, 5081-5092

Stenborg, G. and Cobelli, P. J. 2003, *A&A*, 398, 1185